Middlesex University Research Repository

An open access repository of

Middlesex University research

http://eprints.mdx.ac.uk

This version is available at: https://eprints.mdx.ac.uk/7670/

Iterative (Turbo Processing) Receiver Design of OFDM Systems in The Presence of Carrier Frequency Offset

Huan X. Nguyen [a], Jinho Choi [b] and Huaglory Tianfield [a]

[a] *School of Engineering and Computing, Glasgow Caledonian University, Cowcaddens Road, Glasgow G4 0BA, United Kingdom. Email: {Huan.Nguyen; H.Tianfield}@gcu.ac.uk*

[b] *School of Engineering, Swansea University, Singleton Park, Swansea SA2 8PP, United Kingdom. Email: J.Choi@swansea.ac.uk*

Abstract. In this paper, based on the principle of turbo processing, we propose two iterative receiver schemes for carrier frequency offset (CFO) compensation in orthogonal frequency division multiplexing (OFDM) systems. Our CFO compensation designs, one in time domain and the other in frequency domain, are based on joint estimation of time-varying channel and CFO. In our schemes, the random CFO problem, a challenge for conventional pilot-aid methods, can be effectively solved using iterative (turbo processing) schemes. Furthermore, our comparative study shows that time domain compensation (TDC) is simpler to implement but frequency domain cancellation consisting of an iterative equalizer (FDC-IE) has better bit error rate (BER) performance.

Keywords. Orthogonal frequency division multiplexing (OFDM), turbo processing, carrier frequency offset (CFO), iterative equalizer (IE)

1. Introduction

Orthogonal Frequency Division Multiplexing (OFDM) has been widely used in high data rate wireless communications due to its robustness against multipath fading [1][2]. There are two critical issues in the OFDM receiver design. First, the channel has to be estimated as it is time-varying in real-world environments. Second, since the OFDM signal is very sensitive to carrier frequency offset (CFO) [3], for a receiver to maintain good performance it is essential that CFO is estimated and well compensated.

In the presence of CFO, the orthogonality of subcarriers is lost and as a consequence inter-carrier interference (ICI) has to be considered. To estimate the CFO under perfect knowledge of the channel, cyclic prefix [4] or pilot symbols [5] can be used. However, in practical communication systems, the channel and CFO have to be handled together. Several optimal schemes were proposed for joint estimation of the channel and CFO, including maximum a posteriori (MAP) [6,7], expectation maximization (EM) [8]-[10] and pilot-aided algorithms [11,12]. Other approaches using iterative processing were proposed [13,14] for ICI cancellation. In all these studies, the CFO was considered constant and time-invariant. However, even though it is constant over an OFDM symbol it can be time-varying from symbol to symbol if a spectral mask is deliberately applied to transmitted signals for security reasons (e.g., in military domain [15]). This is similar to the case where a fixed CFO exists along with a random phase noise (PN). In this case, joint estimation, e.g., by exhaustive search, of random CFO and time-varying channel at each time instant is practically impossible. Moreover, pilot symbols are generally inadequate for estimating random CFO. For such circumstance, we believe the turbo processing principle can be applied for CFO estimation, specifically a posteriori data information from the turbo decoder can be utilized.

In this paper, we study two iterative schemes tackling the random CFO problem[1]. The first scheme is time domain compensation (TDC) which is quite simple in implementation and provides an impressive performance. The signal to noise-plus-interference ratio (SINR) is derived with respect to the CFO's estimation error to observe the convergence behaviour after each iteration. We then study frequency domain cancellation which uses an iterative equalizer (FDC-IE) to suppress the ICI caused by CFO. In terms of complexity, FDC-IE is not favoured as complicated algorithmic operations are required to update the IE coefficients. On the other hand, in terms of performance, FDC-IE provides a better bit error rate (BER) performance than TDC. Therefore, we would argue that trade-off between complexity and performance has to be made while choosing between the two schemes TDC and FDC-IE.

The remainder of the paper is organized as follows. In Section 2, OFDM system and channel models are presented. Section 3 presents the time domain CFO compensation scheme on top of the channel estimation. In Section 4, frequency domain CFO compensation using IE is investigated. A comparative analysis of complexity is presented in Section 5. The simulation results are shown in Section 6. Section 7 draws some concluding remarks.

Conventions of notation in the paper are as follows: Boldface upper/lower letters denote matrices/vectors; $(\cdot)^*$, $(\cdot)^T$ and $(\cdot)^H$ denote complex conjugation, transpose and Hermitian transpose, respectively; $\mathrm{Diag}(\mathbf{x})$ (or $\mathrm{Diag}(\mathbf{X})$) represents a diagonal matrix whose diagonal is vector $\mathbf{x}$ (or the diagonal of matrix $\mathbf{X}$); $\mathrm{Tr}(\cdot)$ denotes trace of matrix; $\mathrm{E}[\cdot]$ (or $\mathrm{E}_{\mathbf{x}}[\cdot]$) denotes statistic expectation (or statistic expectation taken with respect to $\mathbf{x}$); $[\mathbf{A}]_{kk'}$ denotes the (k, k')th entry of matrix $\mathbf{A}$; $\Re\{\cdot\}$ denotes the real component; and $\mathcal{C}_L(\mathbf{x})$ denotes circular convolution matrix with L columns ($L \leq$ length of vector $\mathbf{x}$) which are composed of cyclically shifted versions of $\mathbf{x}$.

2. System and Channel Models

This section presents models of the OFDM system and the time-varying channel. A turbo encoder with two recursive systematic convolutional (RSC) encoders is employed for channel coding with a random bit interleaver. For signaling, quadrature phase shift keying (QPSK) is used with constellation set $\mathcal{Q} = \{(\pm 1 \pm j)/\sqrt{2}\}$. The OFDM symbol at time index n is denoted as

$$\mathbf{s}(n) = [s_0(n), s_1(n), \cdots, s_{K-1}(n)]^T \tag{1}$$

where $s_k(n) \in \mathcal{Q}$ is the QPSK symbol at the kth subcarrier and K is the number of subcarriers in an OFDM symbol. For initial estimation of channel and CFO at the receiver, block-type pilot symbols [16] are periodically inserted amongst OFDM data symbols. In order to suppress inter-symbol interference (ISI), a cyclic prefix (CP) consisting of the last L samples of each OFDM symbol is inserted, where L is the channel length.

Consider a time-varying channel whose channel impulse response (CIR) at time t with L multipaths can be written as

$$h(\tau, t) = \sum_{l=0}^{L-1} \gamma_l(t) \delta(\tau - \tau_l) \tag{2}$$

where $\gamma_l(t)$ and τ_l stand for the fading coefficient and delay of the lth multipath component, respectively. Assume the channel is a wide-sense stationary uncorrelated scattering (WSSUS) Rayleigh fading and remains unchanged during one OFDM block interval. We also assume that the maximum channel impulse span is still within the guard interval. For convenience, let $\tau_l = lT_d$ and $T_d = T/K$, where T

---

[1]We focus our discussion on the random CFO only. However, our proposed iterative schemes can readily be extended to the case of constant CFO plus random time-varying PN which is often the case in conventional OFDM systems.

denotes the useful OFDM symbol interval. Let T_s denote the total OFDM symbol interval which is the sum of the useful OFDM symbol interval and the guard interval, i.e., $T_s = T + T_g$, where T_g represents the guard interval. The channel impulse vector at time index n,

$$\mathbf{h}(n) = [h_0(n), h_1(n), \cdots, h_{L-1}(n)]^\mathrm{T}, \tag{3}$$

represents the discrete-time CIR. The autocorrelation function of the CIR $h_l(n) = h(lT_d, nT_s)$ can be expressed as

$$\mathrm{E}[h_l(n)h_{l'}^*(n')] = \sigma_l^2 J_0(2\pi f_D(n - n')T_s)\delta_{ll'} \tag{4}$$

where f_D is the maximum Doppler frequency, $J_0(.)$ the zero order Bessel function of the first kind, $\delta_{ll'}$ the Kronecker delta, and σ_l^2 the normalized average power of each propagation tap, satisfying $\sum_{l=0}^{L-1} \sigma_l^2 = 1$. The urban-like power delay profile [17] is used to model $\{\sigma_l^2\}$. The discrete frequency impulse response vector can be denoted as

$$\bar{\mathbf{h}}(n) = [\bar{h}_0(n), \bar{h}_1(n), \cdots, \bar{h}_{K-1}(n)]^\mathrm{T} \tag{5}$$

where $\bar{h}_k(n) = \sum_{l=0}^{L-1} h_l(n)e^{-j2\pi lk/N}$. The autocorrelation function of the channel frequency response $\bar{h}_k(n) = \bar{h}(k/T, nT_s)$ can be expressed as

$$\mathrm{E}[\bar{h}_k(n)\bar{h}_{k'}^*(n')] = J_0(2\pi f_D(n - n')T_s) \times \sum_{l=0}^{L-1} \sigma_l^2 e^{-\frac{2\pi j}{K}l(k-k')}. \tag{6}$$

At each time instant n we have the correlation matrix $\mathbf{R}_{\bar{\mathbf{h}}\bar{\mathbf{h}}} = \mathrm{E}[\bar{\mathbf{h}}(n)\bar{\mathbf{h}}^\mathrm{H}(n)]$, where

$$[\mathbf{R}_{\bar{\mathbf{h}}\bar{\mathbf{h}}}]_{kk'} = \sum_{l=0}^{L-1} \sigma_l^2 e^{-j2\pi l(k-k')/K}. \tag{7}$$

At the receiver after discarding CP the received signal vectors in time and frequency domains can be expressed as

$$\mathbf{r}(n) = \mathbf{S}(n)\mathbf{h}(n) + \mathbf{w}(n), \tag{8}$$

$$\bar{\mathbf{r}}(n) = \bar{\mathbf{S}}(n)\bar{\mathbf{h}}(n) + \bar{\mathbf{w}}(n) \tag{9}$$

respectively, where $\mathbf{S}(n) = \mathcal{C}_L(\mathbf{F}^\mathrm{H}\mathbf{s}(n))$ and $\bar{\mathbf{S}}(n) = \mathrm{Diag}(\mathbf{s}(n))$. $\mathbf{F}^\mathrm{H}$ is the normalized inverse discrete Fourier transform (IDFT) matrix where $[\mathbf{F}]_{k+1,l+1} = \frac{1}{\sqrt{K}}e^{-j2\pi kl/K}$, $k, l = 0, 1, \ldots, K-1$, comprises the discrete Fourier transform (DFT) matrix. $\mathbf{w}(n)$ and $\bar{\mathbf{w}}(n)$ are the zero-mean time and frequency Gaussian noise vectors, respectively, satisfying $\mathrm{E}[\mathbf{w}(n)\mathbf{w}^\mathrm{H}(n)] = \sigma_w^2\mathbf{I}$ and $\mathrm{E}[\bar{\mathbf{w}}(n)\bar{\mathbf{w}}^\mathrm{H}(n)] = \sigma_{\bar{w}}^2\mathbf{I}$.

In practice, one of the main problems in OFDM receivers is the presence of CFO and random PN as they cause non-orthogonality among subcarriers and consequently cause ICI. In the presence of CFO/PN, Eq. (8) can be rewritten as

$$\hat{\mathbf{r}}(n) = \mathbf{\Psi}(n)\mathbf{S}(n)\mathbf{h}(n) + \mathbf{w}(n) \tag{10}$$

where

$$\mathbf{\Psi}(n) = \mathrm{Diag}([e^{j\theta_1(n)}, e^{j\theta_2(n)}, \cdots, e^{j\theta_K(n)}]) \tag{11}$$

and $\theta_k(n)$ is the phase distortion of the kth subcarrier caused by CFO and/or PN. Considering CFO only, we have $\theta_k(n) = 2\pi\frac{(k-1)\nu(n)}{K}$, where $\nu(n)$ denotes the frequency offset and is usually a constant. However, random CFO can be introduced when a spectral mask is deliberately applied to transmitted signals for security reasons [15]. We consider an extreme case where spectral mask is applied not only to preambles but also to data signals. This implies that CFO can change from one symbol to another. In this case, CFO can be expressed as $\nu(n) = \epsilon + \delta_\epsilon(n)$, where ϵ is a constant offset and $\delta_\epsilon(n)$ a uniformly distributed random offset. This is similar to the case of a fixed CFO plus a random phase noise (PN). Estimating random CFO is a challenging task for conventional pilot-aided approaches as well as joint optimal solutions since random CFO has to be estimated at each time instant. This motivates us to investigate the iterative schemes to tackle this problem as the turbo processing principle can utilize a posteriori data information in addition to pilot signals.

3. CFO Estimation and Time-Domain Compensation

In this section we will design an iterative OFDM receiver to tackle the random CFO problem in the time domain. A block diagram of the iterative receiver is shown in Figure 1. For conciseness, time index n is dropped hereafter. The soft-demapper provides extrinsic information $\bar{L}_k^{(i)}$ of the coded bit $i \in \{0,1\}$ to the turbo decoder [18]. The turbo decoder provides the a posteriori probability (APP) value [19] at bit-level $L_k^{(i)}$ and symbol-level $\Pr(s_k)$ to the soft-damapper and channel and CFO estimators.
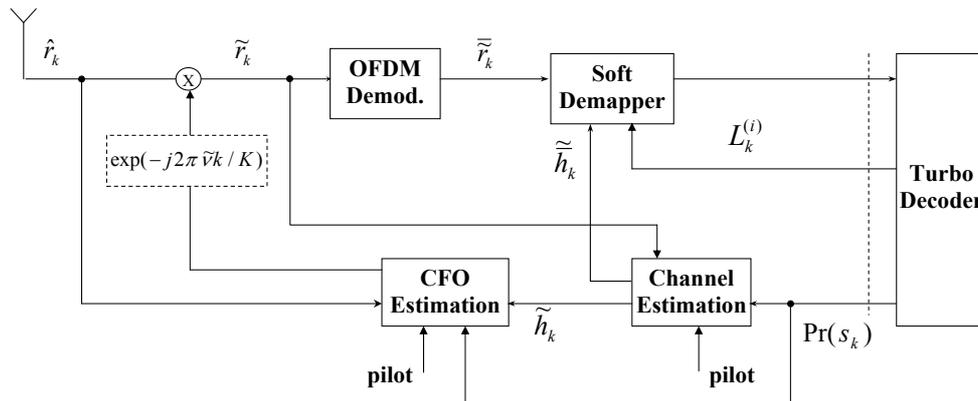

Figure 1. Iterative receiver with channel estimation and CFO's time-domain compensation.

On the first iteration, we use block-type pilot symbols to estimate the channel at pilot symbol positions. The channel is then obtained for the whole time-frequency grid using smoothing [20]. Because the soft information from the decoder is not yet available and pilot symbols alone are not enough to estimate the random CFO at the data symbol positions, we therefore assume the initial CFO $\nu = 0$ at all data symbol positions. From the second iteration onwards, the soft information is already available from the previous iteration and the channel can be re-estimated for use in the CFO estimation. Iterations are detailed in Table 1[2].

Channel estimation is carried out on the assumption that the received signal can already compensate for the CFO at the previous iteration (though there is no compensation at the first iteration.) The channel vector is estimated as

$$\tilde{\mathbf{h}} = \arg\min_{\mathbf{h}} \mathrm{E}_{\mathbf{S}}[\|\mathbf{r} - \mathbf{S}\mathbf{h}\|^2] = \arg\min_{\mathbf{h}} \sum_{\mathbf{S}} \|\mathbf{r} - \mathbf{S}\mathbf{h}\|^2 \Pr(\mathbf{S}). \tag{12}$$

---

[2]For convenience, subscript $(.)_{(m)}$ representing the mth iteration is included in the table.

Table 1. A summary of iterative CFO estimation and compensation

Step	1st iteration	mth iteration ($m \geq 2$)
1	Set initial APP value $L_{k;(0)}^{(i)} = 0$.	Re-estimate channel using the proposed iterative channel estimator, given $\tilde{\mathbf{r}}_{(m-1)}$ and $L_{k;(m-1)}^{(i)}$.
2	Set initial $\nu = 0$. (i.e $\tilde{\boldsymbol{\Psi}}_{(1)} = \mathbf{I}$).	Smooth for better channel estimates: $\hat{\tilde{\mathbf{h}}}_{(m)}$.
3	Estimate channel at pilot symbol positions.	Estimate CFO: $\tilde{\boldsymbol{\Psi}}_{(m)}$ using $\tilde{\mathbf{h}}_{(m)}$, $\hat{\mathbf{r}}$, and $L_{k;(m-1)}^{(i)}$.
4	Obtain channel for the whole grid $\tilde{\mathbf{h}}_{(1)}$ using smoothing.	If the FDC-IE is used, update IE coefficients ($\mathbf{G}_{(m)}$ and $\mathbf{U}_{(m)}$) using $\tilde{\boldsymbol{\Psi}}_{(m)}$ and $\tilde{\mathbf{h}}_{(m)}$.
5	Compensate CFO: $\tilde{\mathbf{r}}_{(1)} = \tilde{\boldsymbol{\Psi}}_{(1)}^{\mathrm{H}} \hat{\mathbf{r}} = \hat{\mathbf{r}}$ (There is actually no compensation at the 1st iteration.)	Compensate CFO: If FDC-IE is used $\mathbf{d}_{(m)} = \mathbf{G}_{(m)}^{\mathrm{H}} \hat{\mathbf{r}} - \mathbf{U}_{(m)}^{\mathrm{H}} \bar{\mathbf{s}}_{(m-1)}$; If TDC is used $\tilde{\mathbf{r}}_{(m)} = \tilde{\boldsymbol{\Psi}}_{(m)}^{\mathrm{H}} \hat{\mathbf{r}}$.
6	Soft demap using $\tilde{\mathbf{h}}_{(1)}$, $\tilde{\mathbf{r}}_{(1)}$, and $L_{k;(0)}^{(i)}$.	Soft demap using $\mathbf{d}_{(m)}$, $L_{k;(m-1)}^{(i)}$ (for FDC-IE scheme) or $\tilde{\mathbf{r}}_{(m)}$, $L_{k;(m-1)}^{(i)}$, $\tilde{\mathbf{h}}_{(m)}$ (for TDC scheme).
7	Update $L_{k;(1)}^{(i)}$ from the decoder.	Update $L_{k;(m)}^{(i)}$ from the decoder.

After some manipulations, we have

$$\tilde{\mathbf{h}} = \left(\mathcal{C}_L(\mathbf{F}^{\mathrm{H}} \mathbf{e}) \right)^{\mathrm{H}} \mathbf{r} \tag{13}$$

where $\mathbf{e} = [e_0, e_1, \cdots, e_{K-1}]^{\mathrm{T}}$, $e_k = \sum_{\rho \in \mathcal{Q}} \rho \Pr(s_k = \rho)$ and $\Pr(s_k = \rho)$ is the a posteriori probability of $s_k = \rho$ which is available from the turbo decoder.

Once channel estimates are available, we can go on to estimate CFO. From (10), the received signal vector can be rewritten as

$$\hat{\mathbf{r}} = \boldsymbol{\Psi} \mathbf{H} \mathbf{F}^{\mathrm{H}} \mathbf{s} + \mathbf{w} \tag{14}$$

where $\mathbf{H} = \mathcal{C}_K(\mathbf{h}_K)$ and the $K \times 1$ vector $\mathbf{h}_K = [h_0, h_1, \cdots, h_{L-1}, 0, \cdots, 0]^{\mathrm{T}}$. Assume that channel matrix $\mathbf{H}$ is available from the channel estimation stage. We now consider a maximum likelihood CFO estimator as follows:

$$\tilde{\nu} = \arg \min_{\nu} \phi(\nu) \tag{15}$$

where

$$\begin{aligned}
\phi(\nu) &= \| \hat{\mathbf{r}} - \boldsymbol{\Psi} \mathbf{H} \mathbf{F}^{\mathrm{H}} \mathrm{E}_{\mathbf{s}}[\mathbf{s}] \|^2 \\
&= \hat{\mathbf{r}}^{\mathrm{H}} \hat{\mathbf{r}} - \mathbf{e}^{\mathrm{H}} \mathbf{F} \mathbf{H}^{\mathrm{H}} \boldsymbol{\Psi}^{\mathrm{H}} \hat{\mathbf{r}} - \hat{\mathbf{r}}^{\mathrm{H}} \boldsymbol{\Psi} \mathbf{H} \mathbf{F}^{\mathrm{H}} \mathbf{e} + \mathbf{e}^{\mathrm{H}} \mathbf{F} \mathbf{H}^{\mathrm{H}} \underbrace{\boldsymbol{\Psi}^{\mathrm{H}} \boldsymbol{\Psi}}_{\mathbf{I}} \mathbf{H} \mathbf{F}^{\mathrm{H}} \mathbf{e} \\
&= -2 \Re \{ \mathbf{e}^{\mathrm{H}} \mathbf{F} \mathbf{H}^{\mathrm{H}} \boldsymbol{\Psi}^{\mathrm{H}} \hat{\mathbf{r}} \} + C \tag{16}
\end{aligned}$$

and C is a constant. The estimator becomes

$$\tilde{\nu} = \arg \max_{\nu} \Re \{ \mathbf{e}^{\mathrm{H}} \mathbf{F} \mathbf{H}^{\mathrm{H}} \boldsymbol{\Psi}^{\mathrm{H}} \hat{\mathbf{r}} \} \tag{17}$$

which can be solved using a gradient-type search algorithm. Once estimated matrix $\tilde{\boldsymbol{\Psi}}$ is available, CFO can be compensated for using TDC scheme as follows

$$\tilde{\mathbf{r}} = \tilde{\boldsymbol{\Psi}}^{\mathrm{H}} \hat{\mathbf{r}}. \tag{18}$$

To analyse the convergence behaviour of the iterative CFO compensation algorithm, we derive SINR before decoding with respect to CFO's estimation error under the assumption that the channel

is perfectly estimated. We define ν_{err} as CFO's estimation error (i.e., $\tilde{\nu} = \nu + \nu_{err}$) and assume that CFO's estimation error is uncorrelated with the channel and $\mathrm{E}[\nu_{err}] = \xi$. From (14) and (18), we have

$$\tilde{\mathbf{r}} = \tilde{\boldsymbol{\Psi}}^{\mathrm{H}}\boldsymbol{\Psi}\mathbf{H}\mathbf{F}^{\mathrm{H}}\mathbf{s} + \tilde{\boldsymbol{\Psi}}^{\mathrm{H}}\mathbf{w} = \mathbf{H}\mathbf{F}^{\mathrm{H}}\mathbf{s} + \boldsymbol{\Upsilon}\mathbf{H}\mathbf{F}^{\mathrm{H}}\mathbf{s} + \tilde{\boldsymbol{\Psi}}^{\mathrm{H}}\mathbf{w} \tag{19}$$

where

$$\boldsymbol{\Upsilon} = \mathrm{Diag}([0, e^{-j2\pi\frac{\nu_{err}}{K}} - 1, \cdots, e^{-j2\pi\frac{(K-1)\nu_{err}}{K}} - 1]). \tag{20}$$

After taking DFT of $\tilde{\mathbf{r}}$, we have

$$\bar{\tilde{\mathbf{r}}} = \mathbf{F}\mathbf{H}\mathbf{F}^{\mathrm{H}}\mathbf{s} + \mathbf{F}\boldsymbol{\Upsilon}\mathbf{H}\mathbf{F}^{\mathrm{H}}\mathbf{s} + \mathbf{F}\tilde{\boldsymbol{\Psi}}^{\mathrm{H}}\mathbf{w} = \bar{\mathbf{H}}\mathbf{s} + \mathbf{F}\boldsymbol{\Upsilon}\mathbf{H}\mathbf{F}^{\mathrm{H}}\mathbf{s} + \mathbf{F}\tilde{\boldsymbol{\Psi}}^{\mathrm{H}}\mathbf{w} \tag{21}$$

where $\bar{\mathbf{H}} = \mathbf{F}\mathbf{H}\mathbf{F}^{\mathrm{H}} = \mathrm{Diag}(\bar{\mathbf{h}})$ according to the diagonalization property of a circulant matrix. Note that $\mathbf{H}\mathbf{H}^{\mathrm{H}} = \mathbf{F}^{\mathrm{H}}\bar{\mathbf{H}}\bar{\mathbf{H}}^{\mathrm{H}}\mathbf{F}$. We define SINR before decoding as follows

$$\gamma = \frac{\mathrm{E}[\|\bar{\mathbf{H}}\mathbf{s}\|^2]}{\mathrm{E}[\|\mathbf{F}\boldsymbol{\Upsilon}\mathbf{H}\mathbf{F}^{\mathrm{H}}\mathbf{s}\|^2] + \mathrm{E}[\|\mathbf{F}\tilde{\boldsymbol{\Psi}}^{\mathrm{H}}\mathbf{w}\|^2]} = \frac{\mathrm{Tr}(\mathrm{E}[\bar{\mathbf{H}}\bar{\mathbf{H}}^{\mathrm{H}}])}{\mathrm{Tr}(\mathrm{E}[\mathbf{F}\boldsymbol{\Upsilon}\mathbf{H}\mathbf{H}^{\mathrm{H}}\boldsymbol{\Upsilon}^{\mathrm{H}}\mathbf{F}^{\mathrm{H}}]) + K\sigma_\omega^2}. \tag{22}$$

With the normalized channel defined in Section 2, it can be seen that $\mathrm{E}[\bar{\mathbf{H}}\bar{\mathbf{H}}^{\mathrm{H}}] = \mathbf{I}$. In addition, $\mathrm{Tr}(\mathbf{F}\mathbf{X}\mathbf{F}^{\mathrm{H}}) = \mathrm{Tr}(\mathbf{X})$ since $\mathbf{F}$ is a unitary matrix. Thus, (22) can be rewritten as

$$\begin{aligned}
\gamma &= \frac{K}{\mathrm{Tr}(\mathrm{E}[\boldsymbol{\Upsilon}\mathbf{F}^{\mathrm{H}}\bar{\mathbf{H}}\bar{\mathbf{H}}^{\mathrm{H}}\mathbf{F}\boldsymbol{\Upsilon}^{\mathrm{H}}]) + K\sigma_\omega^2} \\
&= \frac{K}{\mathrm{Tr}(\mathrm{E}[\boldsymbol{\Upsilon}\boldsymbol{\Upsilon}^{\mathrm{H}}]) + K\sigma_\omega^2} \\
&= \frac{1}{2\left(1 - \frac{1}{K}\sum_{k=0}^{K-1}\cos\frac{2\pi\xi k}{K}\right) + \sigma_\omega^2}.
\end{aligned} \tag{23}$$

Since ξ is reasonably small, SINR is a monotonically decreasing function of ξ as shown in Figure 2 for three values of signal to noise ratios (SNRs) of 3, 4, and 5dB (the simulation parameters are given in Section 6). After each iteration, CFO's estimation error is expected to be smaller, thus leading to a higher SINR. Especially, if CFO's estimation error converges to zero (ideal CFO estimation), then SINR converges to the CFO-free case

$$\gamma_{fr} = \frac{1}{\sigma_\omega^2}. \tag{24}$$

In (23), the undesired term $2\left(1 - \frac{1}{K}\sum_{k=0}^{K-1}\cos\frac{2\pi\xi k}{K}\right)$ is caused by ICI (due to CFO's estimation error). This term is proportional to ξ (for small ξ) and directly affects the performance. If CFO is not well estimated and compensated for, the resultant ξ will be reasonably noticeable and the overall performance will be considerably degraded.

4. CFO's Frequency-Domain Compensation Using Iterative Equalizer (FDC-IE)

Although TDC scheme is simple to implement, it may not be effective since a small CFO's estimation error after direct compensation in time domain can result in a noticeable ICI in frequency domain. Therefore, we investigate our second scheme, called FDC-IE, to see how performance could be improved. In this scheme we attempt to suppress the ICI caused by CFO in frequency domain rather
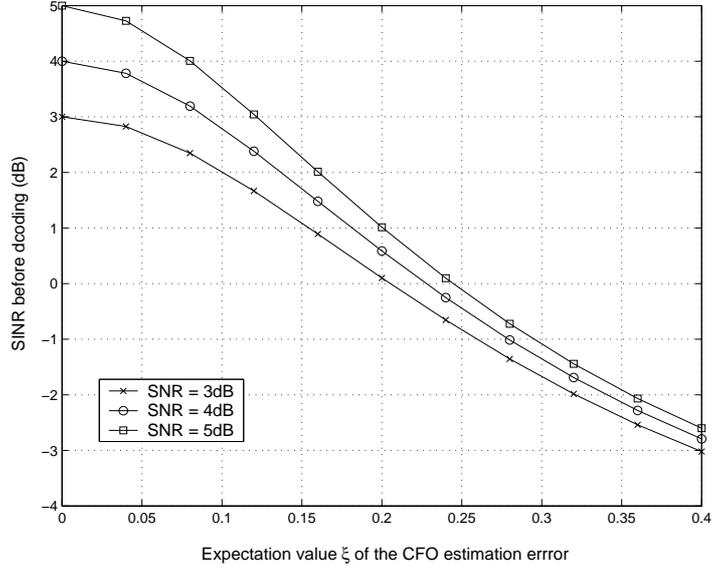
Figure 2. SINR before decoding with respect to the expectation value ξ of CFO's estimation error (in TDC scheme).
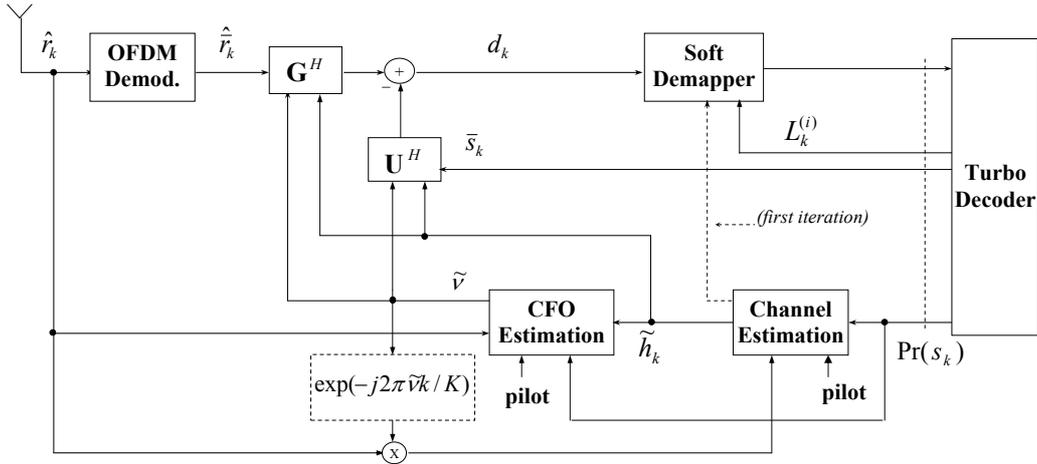

Figure 3. Iterative receiver with channel estimation and frequency-domain CFO compensation using an iterative equalizer.

than directly compensating for CFO in time domain. FDC-IE involves more complicated algorithmic operations but may return better performance as it takes advantage of the frequency-domain iterative equalizer in suppressing ICI and detecting the data symbols.

Figure 3 depicts a block diagram of our proposed FDC-IE scheme. While all the operations are virtually the same as in Section 3, this is a different approach to compensating for CFO. Instead of a direct approach, we use IE to suppress the ICI caused by CFO. Since IE is implemented in frequency domain, DFT operation for OFDM demodulation is only required once for all iterations. After each iteration, better soft information from the turbo decoder will be used to update the coefficients of IE. The iterations are summarised in Table 1. IE's derivation are described as follows.

After taking DFT the received signal in (14) becomes

$$\hat{\bar{\mathbf{r}}} = \mathbf{F}\mathbf{\Psi}\mathbf{H}\mathbf{F}^{\mathrm{H}}\mathbf{s} + \bar{\mathbf{w}} = \mathbf{A}\mathbf{s} + \bar{\mathbf{w}} \tag{25}$$

where $\mathbf{A} = \mathbf{F\Psi HF}^{\mathrm{H}}$.

We employ IE (as illustrated in Figure 3) to make use of the soft decisions from the previous iterations to assist the signal detection at the current iteration. IE's output is given as

$$\mathbf{d} = [d_1, d_2, \cdots, d_K]^{\mathrm{T}} = \mathbf{G}^{\mathrm{H}}\hat{\hat{\mathbf{r}}} - \mathbf{U}^{\mathrm{H}}\bar{\mathbf{s}} \tag{26}$$

where $\mathbf{G}$ is the $K \times K$ filter matrix of FFF, $\mathbf{U}$ is the $K \times K$ filter matrix of the feed-back filter (FBF), and $\bar{\mathbf{s}} = [\bar{s}_1^{\mathrm{T}}, \bar{s}_2^{\mathrm{T}}, \cdots, \bar{s}_K^{\mathrm{T}}]^{\mathrm{T}}$. Here, $\bar{s}_k^{\mathrm{T}}$ is the soft decision of s_k which is available from the decoder. The idea is to design FFF and FBF such that the desired signal component in $\hat{\hat{\mathbf{r}}}$ is preserved and recovered by FFF while ICI is cancelled out as much as possible using FBF. This idea has been used for signal detection in ISI channels [21] and block-iterative detection [22].

The optimal filter matrices $\mathbf{G}$ and $\mathbf{U}$ can be determined using the MMSE criterion as follows

$$\{\mathbf{G}, \mathbf{U}\} = \arg \min_{\{\mathbf{G}, \mathbf{U}\}} \mathrm{E}[\|\mathbf{d} - \mathbf{s}\|^2]$$

$$= \arg \min_{\{\mathbf{G}, \mathbf{U}\}} \mathrm{E}[\|(\mathbf{G}^{\mathrm{H}}\mathbf{A} - \mathbf{I})\mathbf{s} - \mathbf{U}^{\mathrm{H}}\bar{\mathbf{s}} + \mathbf{G}^{\mathrm{H}}\bar{\mathbf{w}}\|^2]. \tag{27}$$

The solution to (27) can be found as

$$\mathbf{G} = (\mathbf{A}\mathbf{Q}\mathbf{A}^{\mathrm{H}} + \sigma_{\bar{w}}^2\mathbf{I})^{-1}\mathbf{A}\mathbf{Q}, \tag{28}$$

$$\mathbf{U} = \mathbf{A}^{\mathrm{H}}\mathbf{G} - \mathbf{I} \tag{29}$$

where $\mathbf{Q} = \mathbf{I} - \mathrm{Diag}([|\bar{s}_1|^2, |\bar{s}_2|^2, \cdots, |\bar{s}_K|^2]^T)$. Note that after each iteration, the soft information from the decoder would be more reliable and matrix $\mathbf{Q}$ would approach further towards $\mathbf{0}$. This means that FFF matrix $\mathbf{G} \to \mathbf{0}$ and FBF matrix $\mathbf{U} \to -\mathbf{I}$ as soft decision vector $\bar{\mathbf{s}} \to \mathbf{s}$.

We now attempt to find SINR at IE's output. The output $\mathbf{d}$ can be rewritten as

$$\mathbf{d} = \mathbf{G}^{\mathrm{H}}\mathbf{A}\mathbf{s} + (\mathbf{I} - \mathbf{G}^{\mathrm{H}}\mathbf{A})\bar{\mathbf{s}} + \mathbf{G}^{\mathrm{H}}\bar{\mathbf{w}} = \mathbf{D}\mathbf{s} + \mathbf{v} \tag{30}$$

where

$$\mathbf{D} = \mathrm{Diag}(\mathbf{G}^{\mathrm{H}}\mathbf{A}) \tag{31}$$

$$\mathbf{v} = (\mathbf{G}^{\mathrm{H}}\mathbf{A} - \mathbf{D})\mathbf{s} + (\mathbf{I} - \mathbf{G}^{\mathrm{H}}\mathbf{A})\bar{\mathbf{s}} + \mathbf{G}^{\mathrm{H}}\bar{\mathbf{w}}. \tag{32}$$

Define $\mathbf{R}_v = \mathrm{E}[\mathbf{v}\mathbf{v}^{\mathrm{H}}]$. We have

$$\mathbf{R}_v = \mathbf{B}\mathbf{B}^{\mathrm{H}} + \mathbf{U}^{\mathrm{H}}\bar{\mathbf{Q}}\mathbf{U} + \sigma_{\bar{w}}^2\mathbf{G}\mathbf{G}^{\mathrm{H}} + \Re\{\mathbf{B}\bar{\mathbf{Q}}\mathbf{U}\} \tag{33}$$

where $\mathbf{B} = \mathbf{G}^{\mathrm{H}}\mathbf{A} - \mathbf{D}$ and $\bar{\mathbf{Q}} = \mathbf{I} - \mathbf{Q}$. SINR of the ith output symbol d_i (where $i = 1, \cdots, K$) becomes

$$\gamma_i = \frac{(\mathbf{g}_i^{\mathrm{H}}\mathbf{a}_i)^2}{[\mathbf{R}_v]_{ii}} \tag{34}$$

where $\mathbf{g}_i$ and $\mathbf{a}_i$ are the ith columns of $\mathbf{G}$ and $\mathbf{A}$, respectively. Since $[\mathbf{R}_v]_{ii} = \mathbf{g}_i^{\mathrm{H}}\mathbf{a}_i - (\mathbf{g}_i^{\mathrm{H}}\mathbf{a}_i)^2$, we can further simplify (34) as

$$\gamma_i = \frac{\mathbf{g}_i^{\mathrm{H}}\mathbf{a}_i}{1 - \mathbf{g}_i^{\mathrm{H}}\mathbf{a}_i}. \tag{35}$$

This SINR function is an increasing function of $\mathbf{g}_i^{\mathrm{H}}\mathbf{a}_i$. At each iteration, new vectors $\mathbf{g}_i^{\mathrm{H}}$ and $\mathbf{a}_i$ are obtained and SINR can be calculated. Numerical depiction in Figure 4 shows the behaviour of the average SINR (taken over all K symbols) for three values of SNR of 3, 4 and 5dB. The average SINR increases after each iteration and converges after six iterations.
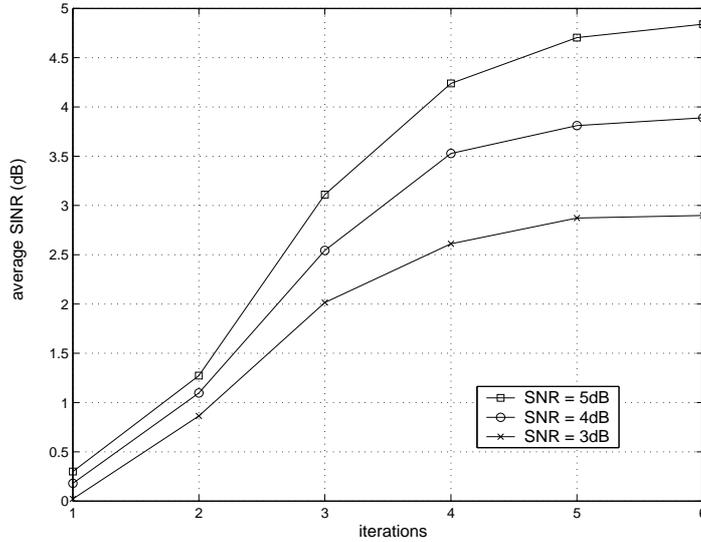
Figure 4. Average SINR at IE's output after each iteration (in FDC-IE scheme) for three SNR values: 3, 4, and 5 dB.

5. Complexity Analysis

The complexity is measured by the number of complex multiplications. We consider only the operations that will result in a difference in implementation between both schemes. Table 2 presents complexity comparison. The exact complexity of the operations such as the fast Fourier transform (FFT) of size K and $K \times K$ matrix inversion can vary depending on their implementations, thus we use them as complexity measurement units: FFT_K denotes the complexity of an FFT operation of size K and $[\cdot]_K^{-1}$ denotes the complexity of inversion operation of a $K \times K$ matrix.

Table 2 shows that TDC scheme has a significant advantage in terms of complexity over FDC-IE scheme. In FDC-IE scheme, we need to update $\mathbf{A}$, $\mathbf{G}$ and $\mathbf{U}$ at each iteration. The inversion of a $K \times K$ matrix required to update FFF coefficient matrix $\mathbf{G}$ contributes significantly to the high complexity. TDC scheme, however, requires only two additional operations - FFT operation for OFDM demodulation and the soft-demaping of the noisy received signal. If we approximate $FFT_K \approx K \log_2 K$, $[\cdot]_K^{-1} \approx K^3$ and choose $K = 64$, we can see the complexity of FDC-IE scheme is significantly (roughly 122 times) higher than that of TDC scheme.

Table 2. Complexity comparison at each iteration

	Updating	Complex multiplications	Total	$K = 64$
FDC-IE	$\mathbf{A}$ $\mathbf{G}$ $\mathbf{U}$	FFT_K $2K^3 + 1\,[.]_{K \times K}^{-1}$ K^3	$3K^3 + FFT_K + 1\,[.]_{K \times K}^{-1}$	1,048,960
TDC	OFDM demod. Soft-demapping	FFT_K $4K^2$	$4K^2 + FFT_K$	8,576

6. Simulation Results

In our simulation, the channel is time-variant and is generated by Jakes' method with Doppler frequency 50Hz. The OFDM system has sixty-four subcarriers with a total bandwidth of 800kHz. QPSK modulation is used. The useful symbol period T is $80\mu s$. The guard interval is one fourth of the useful symbol period, i.e., $T_g = 20\mu s$ with cyclic prefix. The total symbol period becomes $T_s = 100\mu s$. A normal-
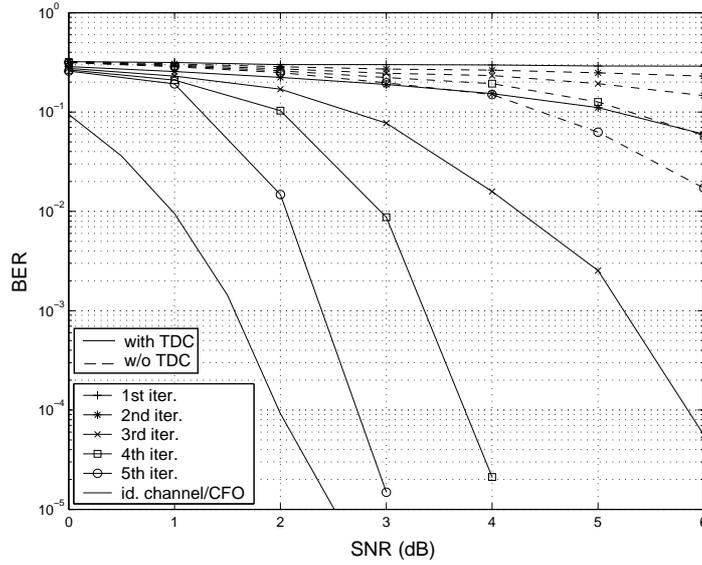
Figure 5. BER performance of the iterative receiver with CFO's time-domain compensation.
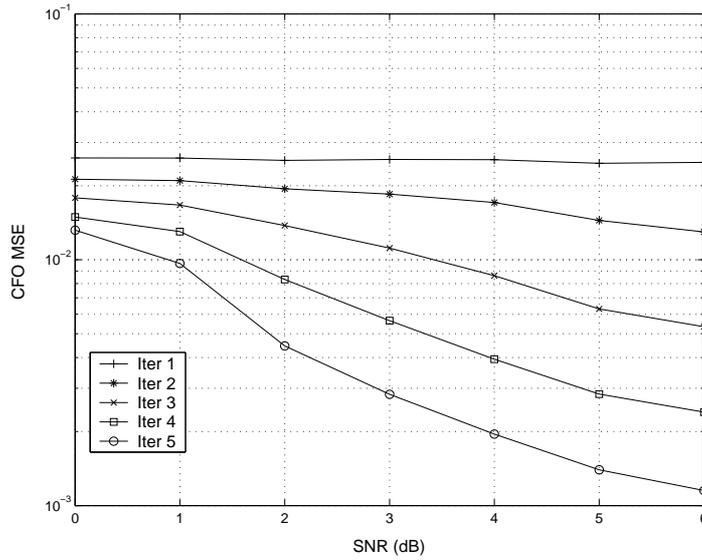

Figure 6. MSE of CFO of the iterative receiver with CFO's time-domain compensation.

ized urban-like power delay profile is assumed. The maximum-delay and the RMS-delay spreads are $13.75\mu s$ and $2.94\mu s$, respectively. A pilot OFDM symbol is inserted at every ten data OFDM symbols. There are 64 OFDM symbols within one OFDM frame in which 6 pilot OFDM symbols are inserted. The turbo code consists of two parallel RSC encoders with generator matrix $\mathbf{P} = (5, 7)$ in octal and a random bit interleaver between them. The receiver becomes doubly-iterative, in which the inner iteration is of the turbo decoder itself with three iterations and the outer one is of the estimation of CFO and channel incorporated by the turbo decoder's soft outputs. CFO is randomly generated as $\nu = \epsilon + \delta_\epsilon$ where $\epsilon = 0.2$ and δ_ϵ is an independently uniformly distributed random offset which is generated in the range of [-0.1, 0.1]. A slow fading channel ($f_D T_s = 0.005$) is considered for simulations. SNR is defined as $1/\sigma_w^2$.
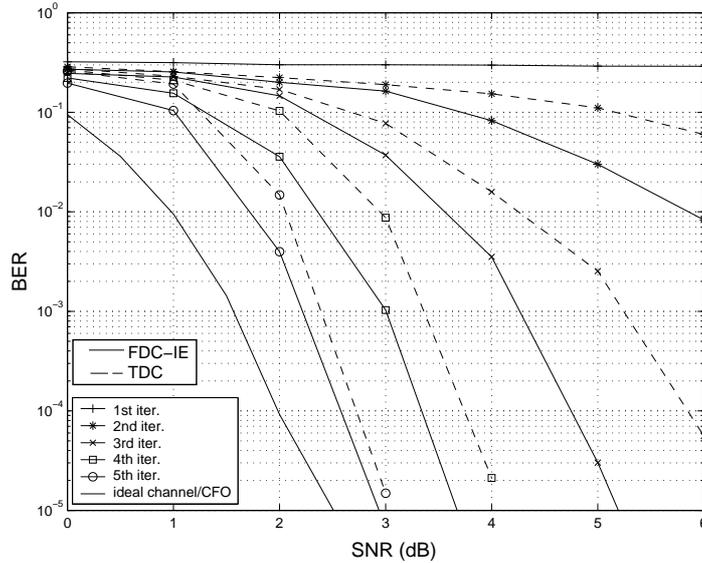
Figure 7. BER performance comparison between CFO's two compensation schemes: TDC versus FDC-IE.

The performance is measured by BER and MSE of CFO obtained after each iteration. MSE of CFO is computed by $MSE = \mathrm{E}[|\tilde{\nu} - \nu|^2]$. Firstly, simulations are carried out to assess the performance of TDC scheme. The BER simulation result is shown in Figure 5. The performance of the first iteration is very poor as CFO is not yet compensated. When CFO estimates are available from the second iteration onwards, the performance is improved significantly after each iteration. For comparison, we consider the case without CFO being compensated while it does exist (dashed curves in Figure 5). It is observed that in the presence of CFO the iterative channel estimator alone provides a very poor performance. However, the performance is improved vastly when the iterative CFO compensation is included along with the channel estimation. The performance at the 5th iteration is not far from the ideal case where there is no CFO and the channel is perfectly known. This draws a remark that our iterative scheme is very effective to solve the random CFO problem. Figure 6 further confirms a significant performance improvement of the MSE of CFO after each iteration.

Secondly, we simulate FDC-IE scheme. In this case, as seen from Table 2, the complexity computation required for FDC-IE scheme is significantly higher than that of TDC scheme. However, a better BER performance is expected. We compare two schemes, TDC (dashed curves) and FDC-IE (solid curves), in Figure 7. The first iteration is the same for both schemes as CFO is not yet compensated. After that, FDC-IE generally outperforms TDC. If the number of iterations is limited, say within two or three iterations, FDC-IE scheme performs rather well and should be chosen though at the expense of higher computational complexity. However, after a certain number of iterations (e.g., by the 5th iteration) there is no significant difference in performance between FDC-IE and TDC, especially at high SNRs. Thus, depending on whether complexity or performance is the main concern, trade-off has to be made while choosing between two schemes.

7. Conclusion

In this paper, we have proposed two iterative (turbo processing) receiver schemes for overcoming CFO problem in OFDM systems. While random, time-varying CFO poses a challenging task for pilot-aided methods for joint estimation of channel and CFO, this can be well solved using our iterative schemes. In particular, from our comparative study on the CFO's time and frequency domain compensation schemes, we have found that an iterative equalizer using decision-feedback processing is highly ef-

fective in suppressing the ICI caused by CFO. The resultant CFO's frequency domain compensation scheme consisting of an iterative equalizer provides better performance than CFO's time domain compensation at the expense of higher complexity. However, the performance gain of CFO's frequency domain compensation does not appear significant while iterations go up. Thus, we would argue that trade off between complexity and performance has to be made while choosing between CFO's time and frequency domain schemes.

References

[1] Cimini LJ. Analysis and simulation of a digital mobile channel using orthogonal frequency division multiplexing. *IEEE Transactions on Communications* 1985; **33**: 665-675.

[2] Sari H, Karam G, Jeanclaude I. Transmission techniques for digital terrestrial TV broadcasting. *IEEE Communications Magazine* 1995; **33**: 100-109.

[3] Pollet T, Van Bladel M, Moeneclaey M. BER sensitivity of OFDM systems to carrier frequency offset and Wiener phase noise. *IEEE Transactions on Communications* 1995; **43**: 191-193.

[4] Van de Beek JJ, Sandell M, Borjesson PO. ML estimation of time and frequency offset in OFDM systems. *IEEE Transactions on Signal Processing* 1997; **45**: 1800-1805.

[5] Yu JH, Su YT. Pilot-assisted maximum-likelihood frequency-offset estimation for OFDM systems. *IEEE Transactions on Communications* 2004; **52**: 1997-2008.

[6] Lin DD, Pacheco RA, Lim TJ, Hatzinakos D. Joint estimation of channel response, frequency offset, and phase noise in OFDM. *IEEE Transactions on Signal Processing* 2006; **54**: 3542-3554.

[7] Barbieri A, Colavolpe G, Caire G. Joint iterative detection and decoding in the presence of phase noise and frequency offset. *IEEE Transactions on Communications* 2007; **55**: 171-179.

[8] Simoens F, Moeneclaey M. Reduced complexity data-aided and code-aided frequency offset estimation for flat-fading MIMO channels. *IEEE Transactions on Wireless Communications* 2006; **5**: 1558-1567.

[9] Sun Y, Xiong Z, Wang X. EM-based iterative receiver design with carrier-frequency offset estimation for MIMO OFDM systems. *IEEE Transactions on Communications* 2005; **53**: 581-586.

[10] Lee JH, Han JC, Kim SC. Joint carrier frequency synchronization and channel estimation for OFDM systems via the EM algorithm. *IEEE Transactions on Vehicular Technology* 2006; **55**: 167-172.

[11] Ma X, Kobayashi H, Schwartz SC. Joint frequency offset and channel estimation for OFDM. In *IEEE 2003 Global Telecommunications Conference*, 2003, pp. 15-19.

[12] Minn H, Al-Dhahir N. Optimal training signals for MIMO OFDM channel estimation in the presence of frequency offset and phase noise. *IEEE Transactions on Communications* 2006; **54**: 1754-1759.

[13] Molish AF, Toeltsch M, Vermani S. Iterative methods for cancellation of intercarier interference in OFDM systems. *IEEE Transactions on Vehicular Technology* 2007; **56**: 2158-2167.

[14] Noels N, Lottici V, Dejonghe A, Steendam H, Moeneclaey M. A theoretical framework for soft-information-based synchronization in iterative (turbo) receiver. *EURASIP Journal on Wireless Communications and Networking* 2005; **2**: 117-129.

[15] Wang X, Ho P, Wu Y. Robust channel estimation and ISI cancellation for OFDM systems with suppressed features. *IEEE Journal on Selected Areas in Communications* 2005; **23**: 963-972.

[16] Coleri S, Ergen M, Puri A, Bahai A. Channel estimation techniques based on pilot arrangement in OFDM systems. *IEEE Transactions on Broadcasting* 2002; **48**: 223-229.

[17] Steele R, *Mobile Radio Communications*, IEEE Press: New York, 1992.

[18] ten Brink S, Speidel J, Yan RH. Iterative demapping for QPSK modulation. *Electronics Letter*, 1998; **34**: 1459-1460.

[19] Hagenauer J, Offer E, Papke L. Iterative decoding of binary block and convolutional codes. *IEEE Transactions on Information Theory* 1996; **42**: 429-445.

[20] Sanzi F, Jelting S, Speidel J. A comparative study of iterative channel estimators for mobile OFDM systems. *IEEE Transactions on Wireless Communications* 2003; **2**: 849-859.

[21] Nguyen XH, Choi J. Decision feedback detection for MIMO-ISI channels: Design using fixed and adaptive constraints. *IEEE Transactions on Vehicular Technology* 2007; **56**: 3931-3937.

[22] Liang YC, Sun S, Ho CK. Block-iterative generalized decision feedback equalizers (BI-GDFE) for large MIMO systems: Algorithm design and asymtotic performance analysis. *IEEE Transactions on Signal Processing* 2006; **54**: 2035-2048.